NASA Technical Memorandum 100164

Effect of High Temperature Annealing on the Microstructure and Thermoelectric Properties of GaP Doped SiGe

Susan L. Draper
Lewis Research Center
Cleveland, Ohio

October 1987

NASA

EFFECT OF HIGH-TEMPERATURE ANNEALING ON THE MICROSTRUCTURE AND THERMOELECTRIC PROPERTIES OF GaP DOPED SiGe

Susan L. Draper
National Aeronautics and Space Administration
Lewis Research Center
Cleveland, Ohio 44135

SUMMARY

Annealing of GaP doped SiGe will significantly alter the thermoelectric properties of the material resulting in increased performance as measured by the figure of merit, Z, and the power factor, P. The microstructures and corresponding thermoelectric properties after annealing in the 1100 to 1300 °C temperature range have been examined to correlate performance improvement with annealing history. The figure of merit and power factor were both improved by homogenizing the material and limiting the amount of cross-doping. Annealing at 1215 °C for 100 hr resulted in the best combination of thermoelectric properties with a resultant figure of merit exceeding 1×10^{-3} °C^{-1} and a power factor of 44 μw cm^{-1} °C^{-2} for the temperature range of interest for space power: 400 to 1000 °C.

INTRODUCTION

The power requirements for future space missions are projected to span the low kilowatt to megawatt power range. The DOD/DOE/NASA SP-100 program is a national effort to develop a family of nuclear reactor space power systems to fulfill a wide range of missions covering these power levels. The baseline space reactor power system technology selected for initial development consists of a lithium-cooled fast reactor and thermoelectric energy conversion (ref. 1).

The thermal energy carried by the reactor coolant is converted to electrical energy by thermoelectric modules utilizing the Seebeck effect. This principle was discovered by Thomas Seebeck who noted that an emf could be produced by purely thermal means in a circuit composed of two different metals whose junctions are maintained at different temperatures (ref. 2). This emf in the circuit is called the Seebeck voltage, V, and a Seebeck coefficient (S) is defined to be proportional to the Seebeck voltage.

$$S = \frac{\partial V}{\partial T} \tag{1}$$

The SP-100 thermoelectric technology will use n- and p-type GaP doped SiGe semiconductors to create the required circuit with a hot side being maintained at 1000 °C by the reactor heat source while the cold side is held near 600 °C through use of heat exchangers and radiation to space. This temperature difference results in heat flow through the two branches of the thermocouple: thus the heat flow is converted to electrical energy which results in current flow through the two legs of the thermocouple. The current flow is utilized by allowing it to flow through an external load.

The effectiveness of the thermoelectric energy conversion is controlled by the Seebeck coefficient (S), electrical resistivity (ρ), and thermal conductivity (Λ). The Seebeck coefficient is affected by the carrier concentration (n), scattering factor (r), and effective mass of an electron (m*), as shown in equation (2) (refs. 3 and 4),

$$S = \left(\frac{k}{e}\right)\left[r + 2 + \ln\left(\frac{Cm^{*3/2}}{n}\right)\right] \tag{2}$$

where k is the Boltzmann constant and C is a constant. The scattering factor is typically 0 for SiGe materials (ref. 3). The efficiency (η) of a thermoelectric device is defined by the electrical output to the load (P_L) and the heat input (q) required to maintain the hot junction temperature (T_h) as shown in equation (3). The electrical output to the load is given by equation (4) where I is the current and R_L is the resistance of the load.

$$\eta = \frac{P_L}{q} \tag{3}$$

$$P_L = I^2 R_L \tag{4}$$

Using the assumptions that the material is homogeneous and S, ρ, and Λ are independent of temperature, the heat flow at the hot junction is determined by three effects: (1) a Peltier heat, q_1, will be absorbed at the hot junction, (2) the hot junction will obtain a portion of the Joule heat, q_2, generated in the elements, and (3) thermal conduction will transport heat, q_3, away from the hot junction. The relationships of these parameters for a temperature differential, $\Delta T = T_h - T_c$, applied across two semiconductor elements, a and b, are:

$$q_1 = -S_{ab} I\, T_h \tag{5}$$

$$q_2 = -\left(\frac{I^2}{2}\right)\left[\rho_a + \left(\frac{\rho_b}{A}\right)\right] L \tag{6}$$

$$q_3 = (\Lambda_a + A\Lambda_b)\frac{\Delta T}{L} \tag{7}$$

$$I = \frac{-S_{ab}\,\Delta T}{\left\{R_L + \left[\rho_a + \left(\frac{\rho_b}{A}\right)\right] L\right\}} \tag{8}$$

where A is the cross-sectional area of element b when element a has unit cross-sectional area and L is the length of each element. The total heat input required to maintain the hot junction temperature is given by a heat balance around the hot junction as shown in equation (9).

$$q = q_1 + q_2 + q_3 \tag{9}$$

Using equations (3) to (9) and maximizing the two parameters A and R_L, the efficiency of a thermoelectric device is given by equation (10).

$$\eta = \frac{\left(\frac{\Delta T}{T_h}\right)\left[(1 + \bar{T}Z)^{1/2} - 1\right]}{\left[(1 + \bar{T}Z)^{1/2} + \frac{T_c}{T_h}\right]} \tag{10}$$

$$\Delta T = T_h - T_c \tag{11}$$

$$\bar{T} = \frac{\left(T_h + T_c\right)}{2} \tag{12}$$

$$Z = \frac{S_{ab}^2}{\left[(\rho_a \Lambda_a)^{1/2} + (\rho_b \Lambda_b)^{1/2}\right]^2} \tag{13}$$

T_h is the hot junction temperature and T_c is the cold junction temperature and $\bar{T}$ is the arithmetical mean temperature. The efficiency of the device is therefore limited by the Carnot efficiency ($\Delta T/T_h$) and depends on the material parameters only through the combination Z, called the figure of merit (ref. 3). These equations refer to a couple; however, a figure of merit for a single material can be defined by equation (14).

$$Z = \frac{S^2}{\rho \Lambda} \tag{14}$$

The power factor (P), defined by equation (15), is also used to measure the performance of a thermoelectric device; however, the effect of the thermal conductivity is not taken into account.

$$P = \frac{S^2}{\rho} \tag{15}$$

From the viewpoint of a space power systems application, it is desirable to minimize system mass. This goal can generally be achieved by maximizing the thermoelectric figure of merit, Z. Early research work on "standard" SiGe performed by Abeles and coworkers (ref. 5) in the 1960's resulted in a Z value of 0.85×10^{-3} K^{-1}; however, subsequent research performed by Pisharody (ref. 6) indicated that doping with GaP decreases the thermal conductivity of SiGe. Unfortunately, the electrical resistivity also increased and therefore the net gain in the figure of merit was small. Raag (ref. 7) observed that annealing the GaP doped SiGe lowered the electrical resistivity, but the samples were not fully characterized.

The investigation reported herein was initiated to determine the effect of annealing on the microstructure and thermoelectric properties of GaP doped SiGe. The temperature and time of annealing was varied and the microstructure characterized using a scanning electron microscope (SEM) with attached energy dispersive spectrometer. The thermoelectric properties were measured and the variation in microstructure was correlated to the observed changes in the thermoelectric properties.

MATERIALS AND EXPERIMENTAL PROCEDURES

The GaP doped SiGe material used was manufactured by Thermo Electron Corporation and has a composition, in atomic percent, of 78.4 Si, 19.6 Ge, and 2.0 GaP. The manufacturing process consisted of hot pressing pure Si and Ge powders, -325 mesh, at 193 MPa for 2 hr in the temperature range of 1150 to 1175 °C. The samples were pulverized, -325 mesh GaP powder added, and hot pressed again using the same parameters. The second pressing increased the homogeneity of the samples. The samples were annealed in air for a variety of temperatures and times as listed in table I. Unfortunately, the annealing temperature was not adequately controlled in all cases so that the temperatures listed with limited certainty were estimated by assessment of the grain size, amount of pitting, and microstructure.

The samples were polished using 0.5 μm diamond as the final polishing agent. Unetched samples were examined in a SEM using a backscattered electron detector (BSE) to characterize the general structure, a x-ray energy dispersive spectrometer to semi-quantitatively measure the compositions, and a wavelength dispersive spectrometer to detect the presence of oxygen. After the SEM analysis, the samples were etched with 30 ml of HNO_3, 10 ml of HF, and 10 ml of H_2O to reveal their grain structure.

The thermoelectric properties of the GaP doped SiGe were measured by the Thermal Power Conversion Group of the Jet Propulsion Laboratory. The Seebeck coefficient, electrical resistivity, and thermal diffusivity were measured up to 1000 °C in existing apparatus at JPL (refs. 8 and 9). The thermal conductivity could not be directly determined, instead it was calculated from equation (16),

$$\Lambda = \alpha C_p p \tag{16}$$

where α is the thermal diffusivity, C_p is the specific heat, and p is the density of the material. The diffusivity apparatus required 1.27-cm diameter disks; however, the life tests (the results of which are not included in this report) required smaller, rod shaped material. Four rods could be obtained from each hot pressed compact only three of which were needed for life tests. To minimize the expense of this investigation, the fourth rod was used for the annealing study. The thermal conductivity could therefore not be measured on several of the samples. The thermal diffusivity was measured on samples T114a and T120 which were annealed with the same schedule as T111 and T118 and therefore were used to calculate the thermal conductivity for these samples. The thermal diffusivity was also measured on sample T178 after annealing at 1275 °C for 8 hr.

MICROSTRUCTURAL RESULTS

The time and temperature of annealing significantly altered the structure of GaP doped SiGe in terms of grain size, chemistry, and phases present. The initial grain size of the material, after a 1165 °C anneal for 24 hr, was 6 μm as shown in table I. While the grain size remained 6 μm after the 100 hr anneal at 1200 °C given sample T111, raising the annealing temperature an additional 15 °C to 1215 °C, for sample T118, caused the grains to grow to 35 μm after 100 hr. The 1275 °C for 8 hr anneal given sample T106 caused a nearly

three-fold increase in grain size. A grain size of 200 μm resulted from holding sample T178 at 1275 °C for 30 hr.

The porosity of these samples was low, on the order of 0.5 percent. Further microstructural characterization revealed that SiO_2 particles were present in all of the samples. While the diameter of the SiO_2 particles was 1 μm or less after 1165 °C heat treatments, these particles grew at higher temperature such that 10 μm diameter particles could be seen following 1275 °C heat treatments. These SiO_2 particles appear as small, dark particles in BSE images as shown in figure 1.

The initial annealing temperature of 1165 °C was not sufficient to homogenize the sample as shown in figure 1. The silicon particles had not completely diffused into the matrix resulting in pure silicon areas, 10 μm in diameter spaced approximately 22 μm apart. GaP particles, shown in figure 2, also remained after annealing. The annealing temperature was raised to 1200 °C to increase the degree of homogenization and the resultant microstructure after 100 hr at 1200 °C is shown in figure 3. Although silicon particles were still present, their separation distance had increased to 300 μm and the GaP particles had completely diffused into the matrix. Raising the annealing temperature to 1215 °C was sufficient to homogenize the sample, as shown in figure 4.

Due to the initial fabrication techniques, the samples had inhomogeneous distributions of Si, Ge, and GaP; thus incipient melting occurred even at the lowest annealing temperature as shown in figure 1. The Ga and P partitioned into the incipient melted areas and upon cooling, a silicon solid solution enriched in Ge, Ga, and P partially surrounded many grains. Diffusion was sufficient at 1215 °C to solidify most of the incipient melted areas during annealing as shown in figure 4 for sample T118. According to the Si-Ge phase diagram, shown in figure 5 (ref. 10), the concentration of Si in the originally melted regions had to be at least 70 at % at 1215 °C to cause this phase change. Remanents of incipient melting are observed to be diffuse layers, approximately 10 μm in thickness, surrounding many grains as shown in figure 4. These layers are slightly enriched in Ge, Ga, and P. The very bright areas in figure 4 have a higher concentration of Ge, Ga, and P. These areas were still liquid when the sample was cooled from the annealing temperature.

Increasing the annealing temperature to 1235 °C for sample T106 increased the overall homogeneity as the incipient melted layers had diffused into the matrix; however, the morphology of the matrix was altered to random variations in composition as shown in figure 6. Each grey level in figure 6 has a slightly different chemical composition. In general, the lighter the image, the higher the Ge, Ga, and P concentration and the darker the image, the higher the Si concentration. The variations in composition do not always correlate with the grain structure. Random variation in chemical distribution were observed in every sample annealed at 1235 °C, or above, except for one side of sample T111 annealed at 1250 °C as shown in figure 7.

Sample T111 was given a series of heat treatments (table I) ending with 8 hr at approximately 1250 °C. The sample had a variation in structure from one side to the other (fig. 7(b)) which could have been due to a temperature gradient in the furnace. The microstructure of the side apparently exposed to a lower annealing temperature had a microstructure similar to sample T118 after a 1215 °C anneal (fig. 7(a)). The incipient melted layer surrounding the

grains was approximately 5 μm in thickness. The right side of the sample, as shown in figure 7(c), had a higher concentration of Ge, Ga, and P with the silicon concentration lower. This side of the sample seems to have been at a higher temperature because the matrix had the random variations in chemistry previously observed in materials annealed at 1235 °C or higher as shown in figure 6.

Annealing at high temperatures resulted in the formation of a (Si,Ge)P phase and what appears to be an eutectic of (Si,Ge)P and (Si,Ge)O_2. These phases are shown in the BSE image of sample T106 annealed at 1275 °C for 8 hr (fig. (8)). The two phase mixture of the eutectic is better illustrated by the optical photomicrograph shown in figure 9. The compositions of these areas were analyzed using a microprobe and the results are given in table II.

The effect of immediately increasing the annealing temperature to 1275 °C following a 1200 °C for 100 hr anneal was explored using sample T178. The resulting microstructure is shown in figure 10. The (Si,Ge)P phase and the eutectic did not form after this annealing schedule. The microstructure was again a random variation in composition, but with a larger variation in composition than observed in sample T106 annealed at 1235 °C.

Sample T178 was annealed at 1275 °C for an additional 30 hr and the resulting microstructure and compositional maps are shown in figure 11. This heat treatment produced a significant amount of liquid phase which was expected based on the temperature, composition, and phase diagram (fig. 5). The melted regions were enriched in Ge and the (Si,Ge)P phase formed upon cooling.

A white powdery phase was observed on the surface of samples annealed at 1235 °C or higher. This was analyzed by x-ray diffraction and determined to be β-Ga_2O_3. The concentration of Ga in the bulk of the samples decreased with increasing time at the higher temperature anneals (table III). Sample T178 after a 1275 °C anneal for 30 hr was completely devoid of Ga.

Ga and P enriched particles, approximately 2 μm in diameter, precipitated in the center of silicon enriched areas. These precipitates were observed in the right side of sample T111 annealed at 1250 °C (fig. 7), sample T106 annealed at 1275 °C for 8 hr (fig. 8), and sample T178 annealed at 1275 °C for 8 hr (fig. 10).

THERMOELECTRIC PROPERTY RESULTS

The effect of annealing on the Seebeck coefficient is shown in figure 12. The Seebeck coefficient was maximized by a 1215 °C annealing temperature for 100 hr, sample T118. The 1225 °C final anneal given sample T111 resulted in the lowest Seebeck coefficient; however, increasing the final annealing step given sample T111 of 1250 °C for 8 hr resulted in significant improvement in the Seebeck coefficient.

A low electrical resistivity is desired for increased performance of thermoelectric devices. The 1275 °C final anneal given sample T106 yielded the lowest resistivity as shown in figure 13. The 1215 °C heat treatment given sample T118 also resulted in a low electrical resistivity. The electrical

resistivity of sample T178 annealed at 1275 °C for 30 hr was very high; therefore, the Seebeck coefficient and thermal conductivity were not measured for this sample.

The thermal conductivity as a function of temperature is plotted in figure 14 for four different annealing schedules; as was the case for resistivity, a low value is desirable for high performance. Sample T120-2, which was annealed at 1215 °C, had the lowest thermal conductivity of the samples measured. As this data was obtained on material given the same heat treatment as sample T118, it could be used to calculate the figure of merit for sample T118. The thermal conductivity for sample T178 annealed at 1275 °C for 8 hr was the highest measured.

The power factor (S^2/ρ) is plotted versus temperature in figure 15. Sample T118, annealed at 1215 °C, had a large power factor due to its high Seebeck coefficient and relatively low electrical resistivity. The low electrical resistivity of sample T106 annealed at 1275 °C also resulted in an attractive power factor. Sample T111, heat treated at 1225 °C, had the lowest power factor due to its poor Seebeck coefficient and electrical resistivity.

The figure of merit, plotted in figure 16, is a function of S, ρ, and Λ. Sample T118 had desirable properties for all three measurements and therefore resulted in a much improved figure of merit over the "standard" SiGe measured by Abeles (ref. 5). The thermal conductivity could not be measured on sample T106; however, the figure of merit was estimated for T106 annealed at 1235 °C from the thermal conductivity data of sample T120-1 annealed at 1225 °C.

A summary of the variations in S, ρ, Λ, and Z are shown in figure 17 for sample T111 annealed at both 1225 °C and 1250 °C. Although the thermal conductivity was lower due to the 1225 °C anneal, the higher S and lower ρ after the 1250 °C anneal outweighed the lower Λ and resulted in a significantly higher Z for the sample annealed at ~1250 °C.

DISCUSSION

The thermoelectric properties of n-type GaP doped SiGe were improved by altering the annealing schedule; however, the reasons for these improvements are not completely understood. A discussion of the correlation of microstructural variations with the observed changes in the thermoelectric properties follows.

Lattice thermal conductivity is decreased by increasing phonon scattering which can be produced by forming solid solutions of silicon and germanium (ref. 6). In order to completely homogenize the GaP doped SiGe in terms of Si-rich islands, GaP particles, and remanents of incipient melting, the annealing temperature had to be at least 1215 °C. Such heat treatments (T118) resulted in a homogeneous microstructure with a few regions of incipient melting, figure 4. In this condition, the Seebeck coefficient was high and the electrical resistivity was low. Such behavior is a contradiction of classical theory which states that the Seebeck coefficient is proportional to the log of the electrical resistivity. Yim and Rosi (ref. 11) have found other n-type material systems to have an increase in Seebeck coefficient after annealing

with a decrease in resistivity. They attributed this result to an increased compositional homogeneity.

Increasing the annealing temperature to 1235 °C for sample T106 resulted in a homogeneous microstructure. The gallium was completely in solution as opposed to sample T118 (1215 °C) in which part of the gallium remained concentrated in the remanents of incipient melting. The Seebeck coefficient was only moderate and the electrical resistivity was fairly high after this anneal. As the electrical resistivity is inversely proportional to the charge carrier concentration and the carrier mobility; cross doping, in which the effective charge carrier concentration is decreased due to the +3 charge of Ga, could be the cause of the high electrical resistivity for this sample. However, the Seebeck coefficient, which was only moderate should have been very high for this sample due to the high level of homogenization.

The thermoelectric properties of sample T111 annealed at approximately 1250 °C could not be related to the microstructure due to the variation in microstructure from one side of the sample to the other.

Sample T106, which had a final anneal at 1275 °C for 8 hr, had good thermoelectric properties. The gallium concentration of this sample decreased considerably due to the vaporization of Ga and the formation of Ga_2O_3 on the surface. Glazov (ref. 12) observed that the addition of Ga increases the solubility limit of P in SiGe. As the Ga vaporized, the solubility of P decreased resulting in the formation of (Si,Ge)P and an eutectic. The P which is tied up as (Si,Ge)P is not contributing to the charge carrier concentration, but there was still sufficient P in solution to have a high concentration of charge carriers. The effect of cross-doping was minimized due to the decreased level of gallium. The grain size of this sample had increased to 70 μm as a result of the annealing. This increase in grain size may also have increased the mobility of charge carriers due to a reduction in grain boundary scattering. The small amount of cross-doping and the large grain size led to a low value for the electrical resistivity while the Seebeck coefficient was high due to the good level of homogenization. Unfortunately, the thermal conductivity could not be measured for this sample so a figure of merit could not be calculated.

Sample T178 was not step annealed to its final annealing temperature; it was annealed at only 1200 °C for 100 hr and then 1275 °C for 8 hr. This heat treatment was not sufficient to vaporize the gallium, therefore, the (Si,Ge)P phase did not form. Incomplete chemical homogenization resulted in a high electrical resistivity and a low Seebeck coefficient. Exposing the sample to an additional 30 hr at 1275 °C resulted in significant melting. The phosphorous was completely tied up in (Si,Ge)P which led to a very high electrical resistivity.

When low frequency phonons, which contribute substantially to the thermal conductivity of a material, are scattered by grain boundaries, the thermal conductivity is decreased (ref. 13). The thermal conductivity is therefore reduced by a fine grained material. Decreases in the thermal conductivity of thermoelectrics can also be made by homogenizing the material as noted by Airapetiants (ref. 14) who stated that compositional inhomogeneities caused circulating currents which not only lowered the Seebeck coefficient but also enhanced the transport of heat. These two theories were substantiated by the results of this investigation where the thermal conductivity of sample T118

annealed at 1215 °C was low due to its homogeneity and small grain size. The homogeneity of sample T111 annealed at 1250 °C outweighed the effect of sample T178's small grain size resulting in the lower thermal conductivity measurements for sample T111. The homogeneity of the sample appears to be the dominant factor for low thermal conductivity.

SUMMARY

The effect of annealing on the microstructure and thermoelectric properties of GaP doped SiGe were characterized in this investigation. A 1215 °C anneal was needed to properly diffuse the silicon and GaP particles into the matrix. Significant grain growth was observed for samples annealed above 1200 °C. The loss of gallium by vaporization decreased the solubility of P in the matrix and led to the formation of (Si,Ge)P when samples were annealed at 1250 °C or higher.

Thermoelectric materials with high power factors can be obtained by annealing SiGe doped with GaP at 1215 °C for 100 hr, or step annealing to 1275 °C (sample T106). A multiple step heat treatment schedule appears to be important, as raising the annealing temperature to 1275 °C after only a 1200 °C anneal resulted in an inhomogeneous material with poor thermoelectric properties. The presence of Ga increased the solubility limit of P in SiGe; however, the concentration of Ga in solution should be limited to minimize the amount of cross-doping. This limit can be achieved by vaporizing the Ga to form β-Ga_2O_3 on the surface or by concentrating it in the incipient melted regions. In either case the amount of cross-doping is limited. The Seebeck coefficient was found to increase with a decrease in electrical resistivity. Homogeneity of the sample was the dominant factor for low thermal conductivity. Annealing at 1215 °C for 100 hr resulted in a figure of merit of over 1×10^{-3} K^{-1} and a power factor of 44 $\mu w\ cm^{-1}\ °C^{-2}$ over the operating temperature range: 400 to 1000 °C.

REFERENCES

1. Given, R.W.; Morgan, R.E.; and Chi, J.W.H.: SP-100 Space Nuclear Power System. Advanced Energy Systems - Their Role in Our Future (19th IECEC), vol. 4, American Nuclear Society, LaGrange Park, IL, 1984, pp. 2392-2397.

2. Sears, F.W.; Zemansky, M.W.; and Young, H.D.: University Physics, 5th edition, Addison Wesley Pub. Co., 1976.

3. Heikes, R.R. and Ure, R.W., Jr.: Thermoelectricity: Science and Engineering, Interscience Publishers, 1961.

4. Harman, T.C. and Honig, J.M.: Thermoelectric and Thermomagnetic Effects and Applications, McGraw-Hill, 1967.

5. Abeles, B, et al.: Thermal Conductivity of Ge-Si Alloys at High Temperatures. Phys. Rev., vol. 125, no. 1, Jan. 1, 1982, pp. 44-46.

6. Pisharody, R.K. and Garvey, L.P.: Modified Silicon-Germanium Alloys with Improved Performance. Proceedings of the 13th Intersociety Energy Conversion Engineering Conference, vol. 3, SAE, Warrendale, PA, 1978, pp. 1963-1968.

7. Raag, V.: Unpublished research.

8. Wood, C.; Zoltan, D.; and Stapfer, G.: Measurement of Seebeck Coefficient Using a Light Pulse. Rev. Sci. Instrum., vol. 55, no. 5, May 1985, pp. 719-722.

9. Vandersande, J.W.; Wood, C.; Zoltan, A.; and Whittenberger, D.: to be published in Proceedings of the 19th International Thermal Conductivity Conference, Cookeville, TN, 1985. (Plenum, 1987)

10. Hansen, M.: Constitution of Binary Alloys, Second Edition, McGraw-Hill, 1958, p. 774.

11. Yim, W.M. and Rosi, F.D.: Compound Tellurides and Their Alloys for Peltier Cooling - A Review. Solid State Electron., vol. 15, no. 10, Oct. 1972, pp. 1121-1140.

12. Glazov, V.M. and Zemskov, V.S.: Physiochemical Properties of Semiconductor Doping. Israel Program for Scientific Translations, Jerusalem, 1968.

13. Rowe, D.M. and Shukula, V.S.: The Effect of Phonon-Grain Boundary Scattering on the Lattice Thermal Conductivity and Thermoelectric Conversion Efficiency of Heavily Doped Fine-Grained, Hot-Pressed Silicon Germanium Alloy. J. Appl. Phys., vol. 52, no. 12, Dec. 1981, pp. 7421-7426.

14. Airapetiants, C.V.: Thermal Electromotive Force and Additional Thermal Conductivity of Statistical Mixtures. Sov. Phys. Tech. Phys., vol. 2, no. 2, Feb. 1957, pp. 429-433.

TABLE I. - TIMES AND TEMPERATURES OF ANNEALING AND RESULING GRAIN SIZE

Sample	Temperature, °C	Time, hr	Microstructure characterized	T.E. properties measured	Grain size, μm
T114	1100	24	-	-	---
	1165	24	X	-	6
T106	1165	24	-	-	---
	1200	100	-	-	---
	1207	12	-	-	---
	1235	12	X	X	25
	1275	8	X	X	70
T111	1165	24	-	-	---
	1200	100	X	-	6
	1225	24	-	X	---
	[a]1250	8	X	X	90
T118	1165	24	-	-	---
	[a]1215	100	X	X	35
T178	1200	100	-	-	---
	1275	8	X	X	60
	1275	30	X	X	200

[a]Estmated temperature based on microstructural examination.

TABLE II. - COMPOSITION OF (Si,Ge)P AND EUTECTIC IN ATOMIC PERCENT

	Si	Ge	P	O
Eutectic	40.0	7.3	33.3	19.4
(Si,Ge)P	41.1	11.8	42.6	4.5

TABLE III. - Ga CONCENTRATION IN SOLUTION AFTER ELEVATED TEMPERATURE ANNEALING

Sample	Time, hr	Temperature, °C	Ga/Si, EDS counts
T106	12	1235	0.0154
T106	8	1275	.0025
T178	8	1275	.0159
T178	30	1275	.0000

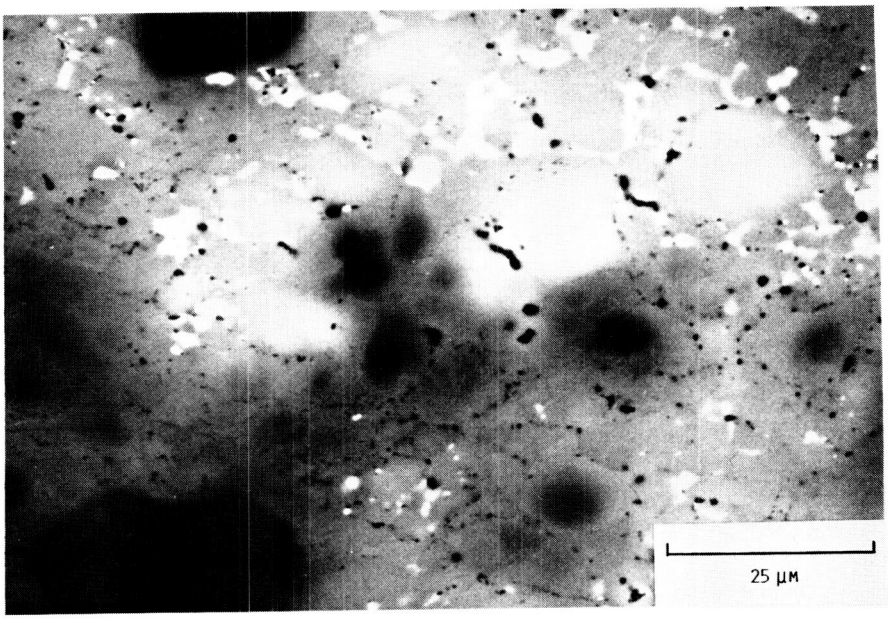

FIGURE 1. - THE MICROSTRUCTURE OF SAMPLE T114 AFTER ANNEALING AT 1100 ^{o}C FOR 24 HR AND 1165 ^{o}C FOR 24 HR. THE Si PARTICLES ARE THE DIFFUSE DARK PARTICLES; SiO_2 PARTICLES ARE SMALL, DARK PARTICLES; AND THE INCIPIENT MELTED AREAS ARE THE LIGHT AREAS OUTLINING GRAINS.

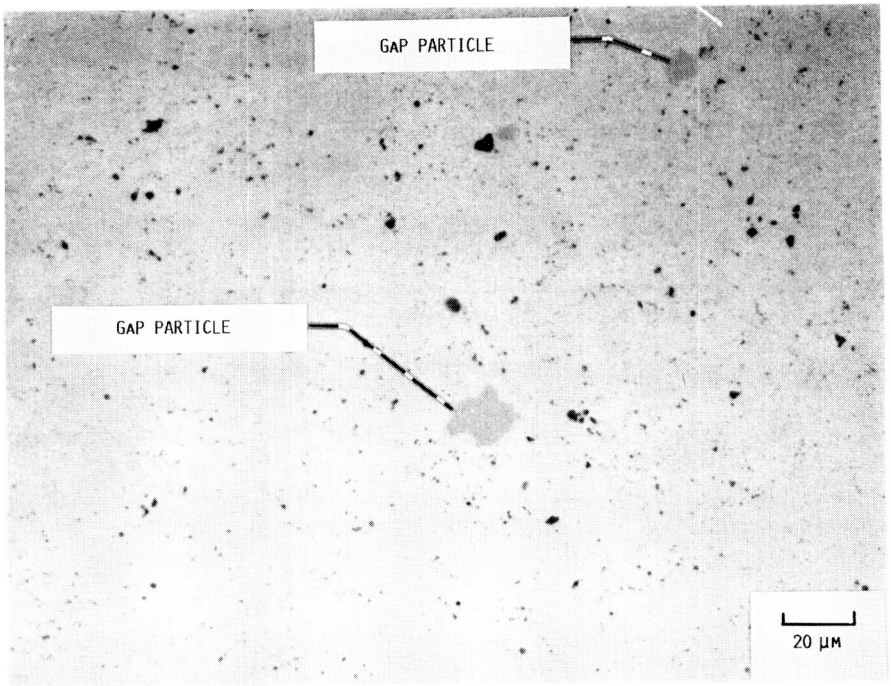

FIGURE 2. - GaP PARTICLES PRESENT IN SAMPLE T114 AFTER ANNEALING AT 1100 ^{o}C FOR 24 HR AND 1165 ^{o}C FOR 24 HR.

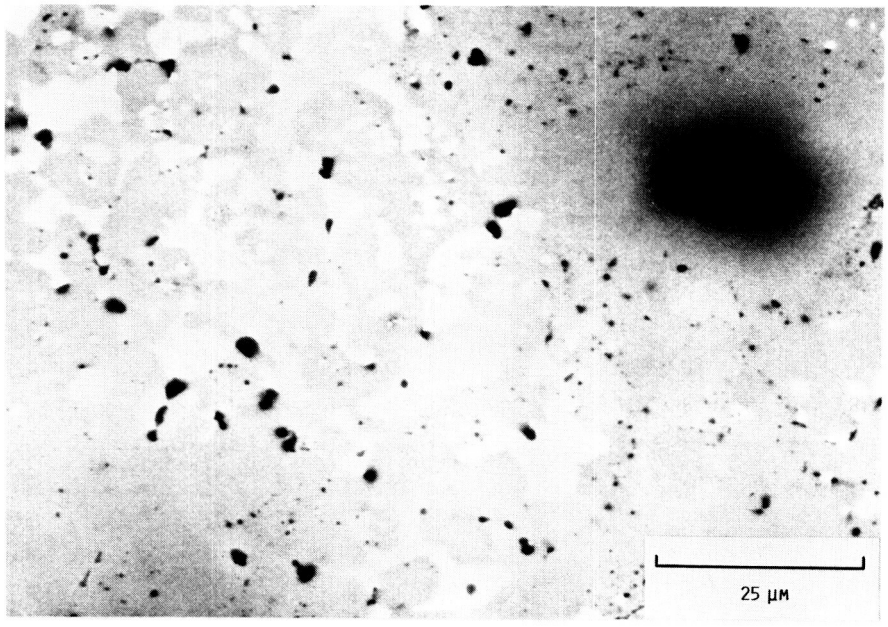

FIGURE 3. - THE MICROSTRUCTURE OF SAMPLE T111 AS A RESULT OF ANNEALING AT 1165 ^{o}C FOR 24 HR AND 1200 ^{o}C FOR 100 HR.

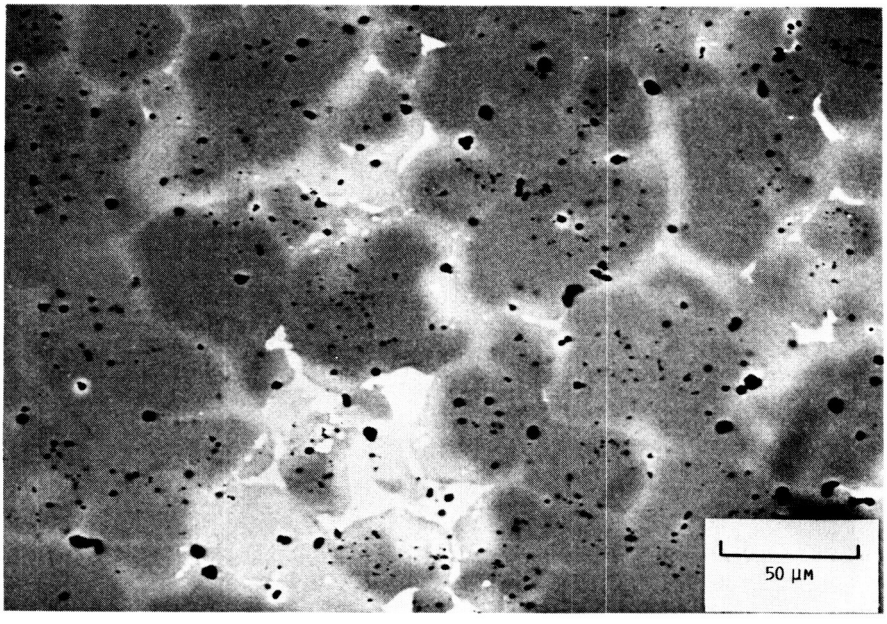

FIGURE 4. - THE MICROSTRUCTURE OF SAMPLE T118 AS A RESULT OF ANNEALING AT 1165 ^{o}C FOR 24 HR AND ~1215 ^{o}C FOR 100 HR.

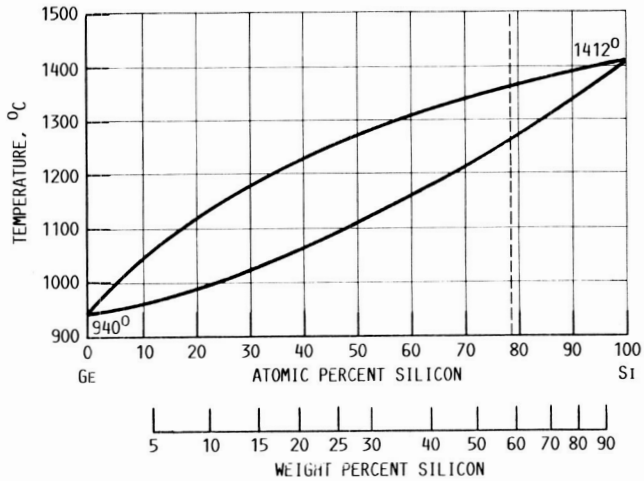

FIGURE 5. - Si-Ge PHASE DIAGRAM [10].

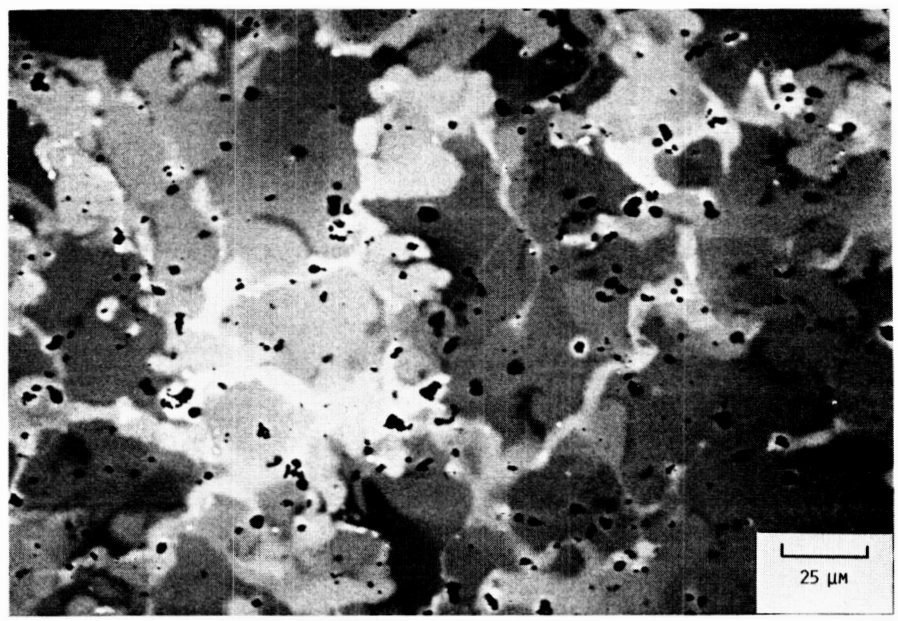

FIGURE 6. - THE MICROSTRUCTURE OF SAMPLE T106 AFTER ANNEALING AT 1165 °C FOR 24 HR, 1200 °C FOR 100 HR, 1207 °C FOR 12 HR, AND 1235 °C FOR 12 HR.

(A) MICROSTRUCTURE OF LEFT SIDE.

(B) LOW MAGNIFICATION BSE IMAGE OF SAMPLE.

(C) MICROSTRUCTURE OF RIGHT SIDE.

FIGURE 7. - THE MICROSTRUCTURE OF SAMPLE T111 AFTER ANNEALING AT 1165 ^{o}C FOR 24 HR, 1200 ^{o}C FOR 100 HR, 1225 ^{o}C FOR 24 HR, AND ~1250 ^{o}C FOR 8 HR.

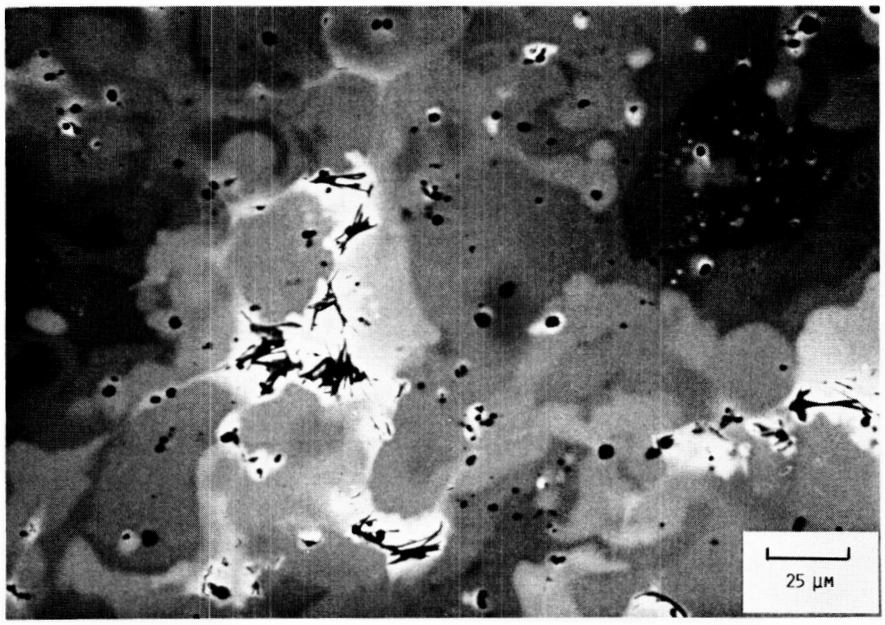

FIGURE 8. - MICROSTRUCTURE OF SAMPLE T106 AFTER ANNEALING AT 1165 ^{O}C FOR 24 HR, 1200 ^{O}C FOR 100 HR, 1207 ^{O}C FOR 12 HR, 1235 ^{O}C FOR 12 HR, AND 1275 ^{O}C FOR 8 HR.

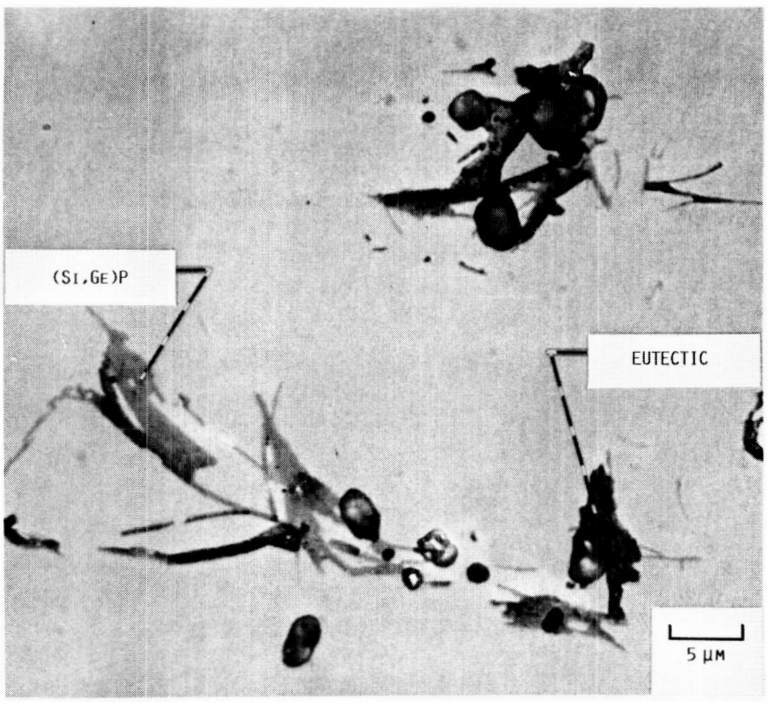

FIGURE 9. - (Si,Ge)P AND AN EUTECTIC OF POSSIBLY (Si,Ge)P AND (Si,Ge)O_2 FORM AFTER ANNEALING AT 1250 ^{O}C.

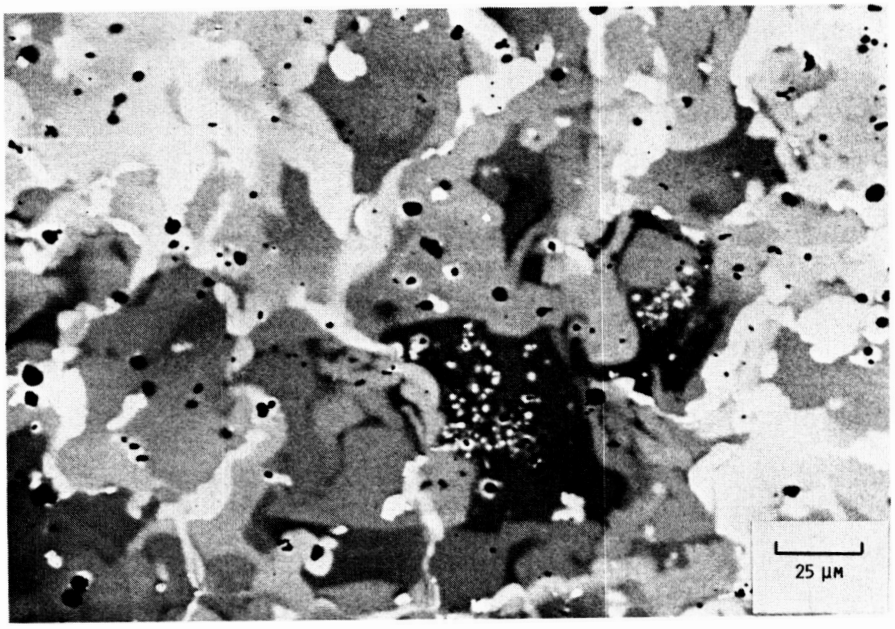

FIGURE 10. - MICROSTRUCTURE OF SAMPLE T178 AFTER ANNEALING AT ONLY 1200 ^{o}C FOR 100 HR AND 1275 ^{o}C FOR 8 HR.

(A) MICROSTRUCTURE.

(B) Si DOT MAP.

(C) Ge DOT MAP.

(D) P DOT MAP.

FIGURE 11. - SEGREGATION OF ELEMENTS DUE TO PARTIAL MELTING OF SAMPLE T178 AFTER ANNEALING AT 1275 ^{0}C FOR 30 HR ARE SHOWN.

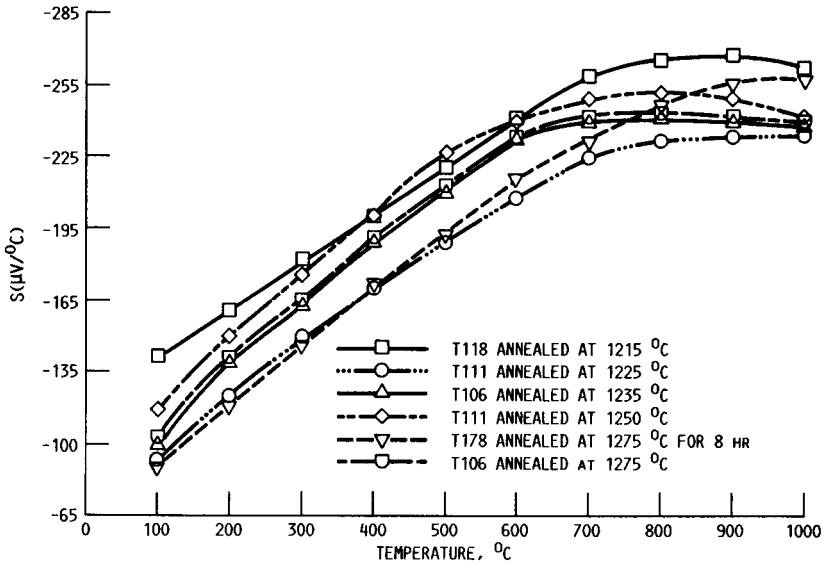

FIGURE 12. - SEEBECK COEFFICIENT OF ANNEALED N-TYPE SiGe/GaP AS A FUNCTION OF TEMPERATURE.

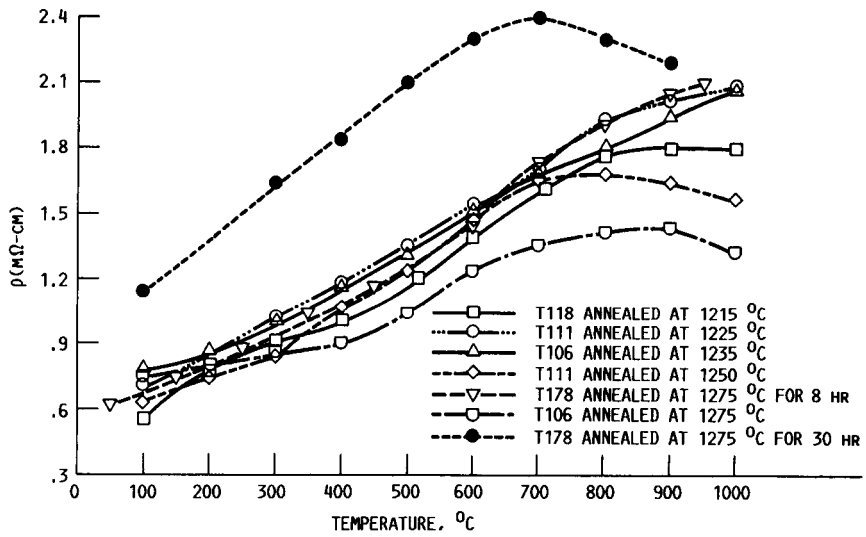

FIGURE 13. - ELECTRICAL RESISTIVITY OF ANNEALED N-TYPE SiGe/GaP AS A FUNCTION OF TEMPERATURE.

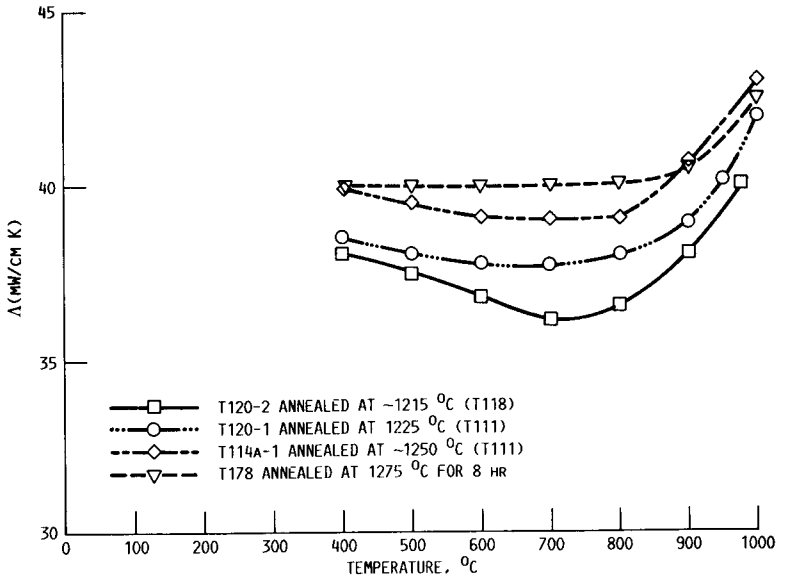

FIGURE 14. - THERMAL CONDUCTIVITY OF ANNEALED N-TYPE SiGe/GaP AS A FUNCTION OF TEMPERATURE.

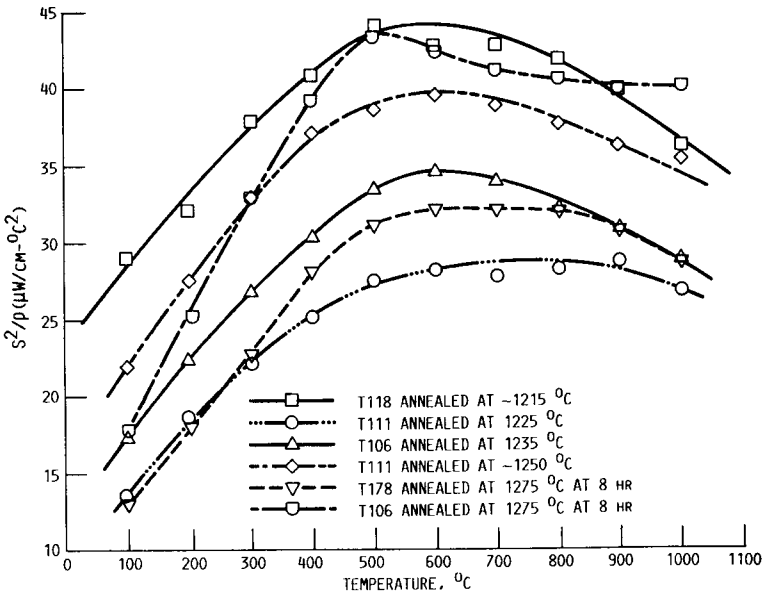

FIGURE 15. - POWER FACTOR, P, OF ANNEALED N-TYPE SiGe/GaP AS A FUNCTION OF TEMPERATURE.

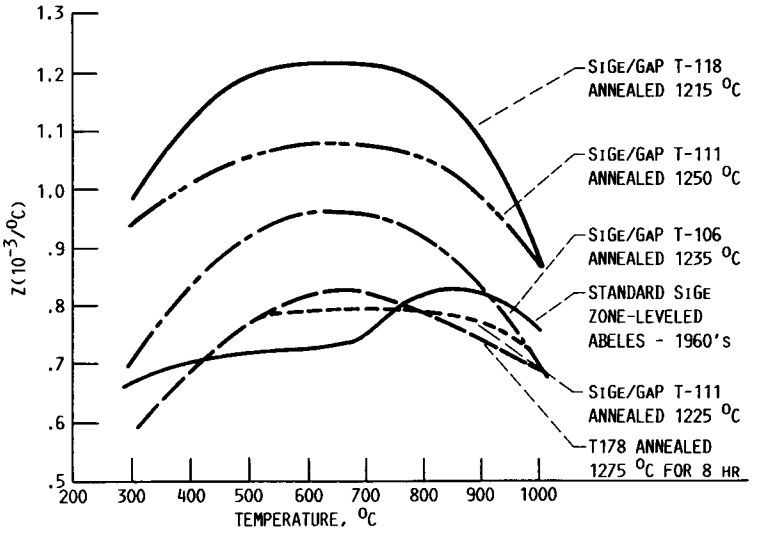

FIGURE 16. - FIGURE OF MERIT, Z, OF ANNEALED N-TYPE SiGe/GaP AS A FUNCTION OF TEMPERATURE.

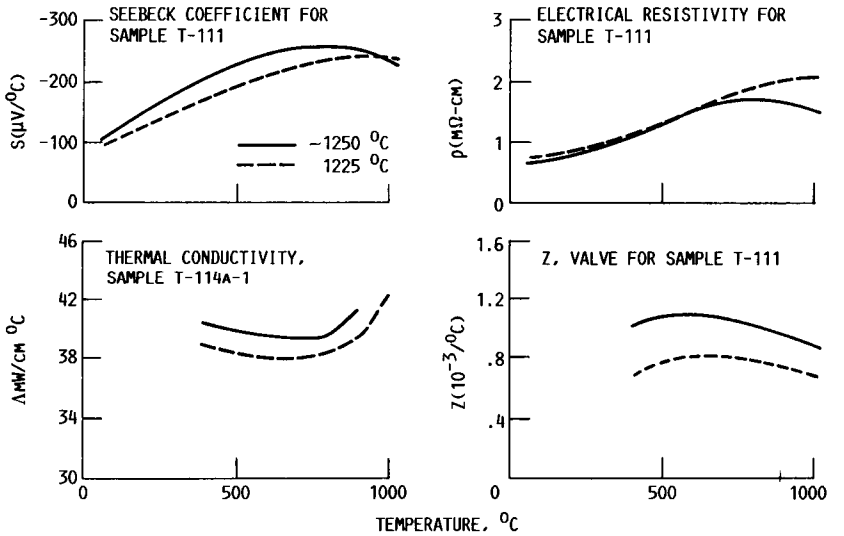

FIGURE 17. - SUMMARY OF THERMOELECTRIC PROPERTIES AS A FUNCTION OF TEMPERATURE FOR SAMPLE T111 AFTER ANNEALING AT 1225 °C AND ~1250 °C.

NASA
National Aeronautics and Space Administration

Report Documentation Page

1. Report No.	2. Government Accession No.	3. Recipient's Catalog No.
NASA TM-100164		

4. Title and Subtitle	5. Report Date
Effect of High-Temperature Annealing on the Microstructure and Thermoelectric Properties of GaP Doped SiGe	October 1987
	6. Performing Organization Code
7. Author(s)	8. Performing Organization Report No.
Susan L. Draper	E-3729
	10. Work Unit No.
	506-41-31
9. Performing Organization Name and Address	11. Contract or Grant No.
National Aeronautics and Space Administration Lewis Research Center Cleveland, Ohio 44135-3191	
	13. Type of Report and Period Covered
12. Sponsoring Agency Name and Address	Technical Memorandum
National Aeronautics and Space Administration Washington, D.C. 20546-0001	14. Sponsoring Agency Code

15. *Supplementary Notes*

This report was a thesis submitted in partial fulfillment of the requirements for the degree Master of Science in Materials Science and Engineering to Case Western Reserve University, Cleveland, Ohio in April 1987.

16. Abstract

Annealing of GaP doped SiGe will significantly alter the thermoelectric properties of the material resulting in increased performance as measured by the figure of merit, Z, and the power factor, P. The microstructures and corresponding thermoelectric properties after annealing in the 1100 to 1300 °C temperature range have been examined to correlate performance improvement with annealing history. The figure of merit and power factor were both improved by homogenizing the material and limiting the amount of cross-doping. Annealing at 1215 °C for 100 hr resulted in the best combination of thermoelectric properties with a resultant figure of merit exceeding 1×10^{-3} °C^{-1} and a power factor of 44 μW cm^{-1} °C^{-2} for the temperature range of interest for space power: 400 to 1000 °C.

17. Key Words (Suggested by Author(s))	18. Distribution Statement
Thermoelectric SiGe Microstructure	Unclassified - Unlimited Subject Category 27

19. Security Classif. (of this report)	20. Security Classif. (of this page)	21. No of pages	22. Price*
Unclassified	Unclassified	22	A02

NASA FORM 1626 OCT 86

*For sale by the National Technical Information Service, Springfield, Virginia 22161